


SCIENTIFIC REPORTS



OPEN

Estrogen receptor α /HDAC/NFAT axis for delphinidin effects on proliferation and differentiation of T lymphocytes from patients with cardiovascular risks

Ousama Dayoub¹, Soazig Le Lay¹ , Raffaella Soleti¹, Nicolas Clere¹, Gregory Hilairat¹, Séverine Dubois^{1,2}, Frédéric Gagnadoux^{1,3}, Jérôme Boursier^{4,5}, Maria Carmen Martínez¹ & Ramaroson Andriantsitohaina¹

Delphinidin, an anthocyanin present in red wine, has been reported to preserve the integrity of endothelium *via* an estrogen receptor alpha (ER α)-dependent mechanism. However, the effect of delphinidin on the immune response in obesity-related inflammation remains unknown. Given the important role of T lymphocytes in obesity-related inflammation, we investigated the effect of delphinidin on proliferation and differentiation of T lymphocytes from healthy subjects and metabolic syndrome patients. Delphinidin decreased the proliferation stimulated by different agents acting through different mechanisms. This effect of delphinidin was associated with its ability to inhibit Ca²⁺ signaling *via* reduced store-operated Ca²⁺ entry and release, and subsequent decrease of HDAC and NFAT activations. Delphinidin also inhibited ERK1/2 activation. Pharmacological inhibition of ER with fulvestrant, or deletion of ER α , prevented the effect of delphinidin. Further, delphinidin suppressed the differentiation of T cells toward Th1, Th17 and Treg without affecting Th2 subsets. Interestingly, delphinidin inhibited both proliferation and differentiation of T cells taken from patients with cardiovascular risks associated with metabolic syndrome. Together, we propose that delphinidin, by acting on ER α *via* multiple cellular targets, may represent a new approach against chronic inflammation associated with T lymphocyte activation, proliferation and differentiation, in patients with cardiovascular risk factors.

Obesity and its metabolic complications including metabolic syndrome (MetS) share a common pathogenic denominator of chronic, low-grade inflammation^{1,2}. These disorders are characterized by a continuous activation of several immune cells including T lymphocytes¹. Activated T lymphocytes play a fundamental role in initiation and development of chronic inflammatory responses. Indeed, increased numbers of T lymphocytes and a modification in the balance between pro-inflammatory (Th1 and Th17 lymphocytes) and anti-inflammatory (Th2 and Treg lymphocytes) CD4⁺ cells subsets have been observed in adipose tissue of obese and MetS patients^{3,4}. Moreover, suppressing of T cell activation protects against obesity and adipose tissue inflammation⁵.

Activation of T lymphocytes through T-cell receptor (TCR) phosphorylates and promotes the translocation of extracellular signal-regulated kinase 1/2 (ERK1/2) into the nucleus to regulate the transcription of target genes⁶. In addition, TCR activation induces an increase in intracellular Ca²⁺ concentration ([Ca²⁺]_i). The increase of [Ca²⁺]_i includes the release of Ca²⁺ from the endoplasmic reticulum *via* the inositol 1, 4, 5-triphosphate (IP₃) production and the store-operated Ca²⁺ entry (SOCE) through Ca²⁺ release-activated Ca²⁺ (CRAC) channels⁷. The

¹INSERM UMR1063, UNIV Angers, Université Bretagne Loire, Angers, France. ²Service d'Endocrinologie Diabétologie Nutrition, Centre hospitalier universitaire, Angers, France. ³Département de Pneumologie, Centre hospitalier universitaire, Angers, France. ⁴Service d'Hépatogastroentérologie, Centre hospitalier universitaire, Angers, France. ⁵Laboratoire HIFIH UPRES EA3859, UNIV Angers, Université Bretagne Loire, Angers, France. Correspondence and requests for materials should be addressed to R.A. (email: ramaroson.andriantsitohaina@univ-angers.fr)

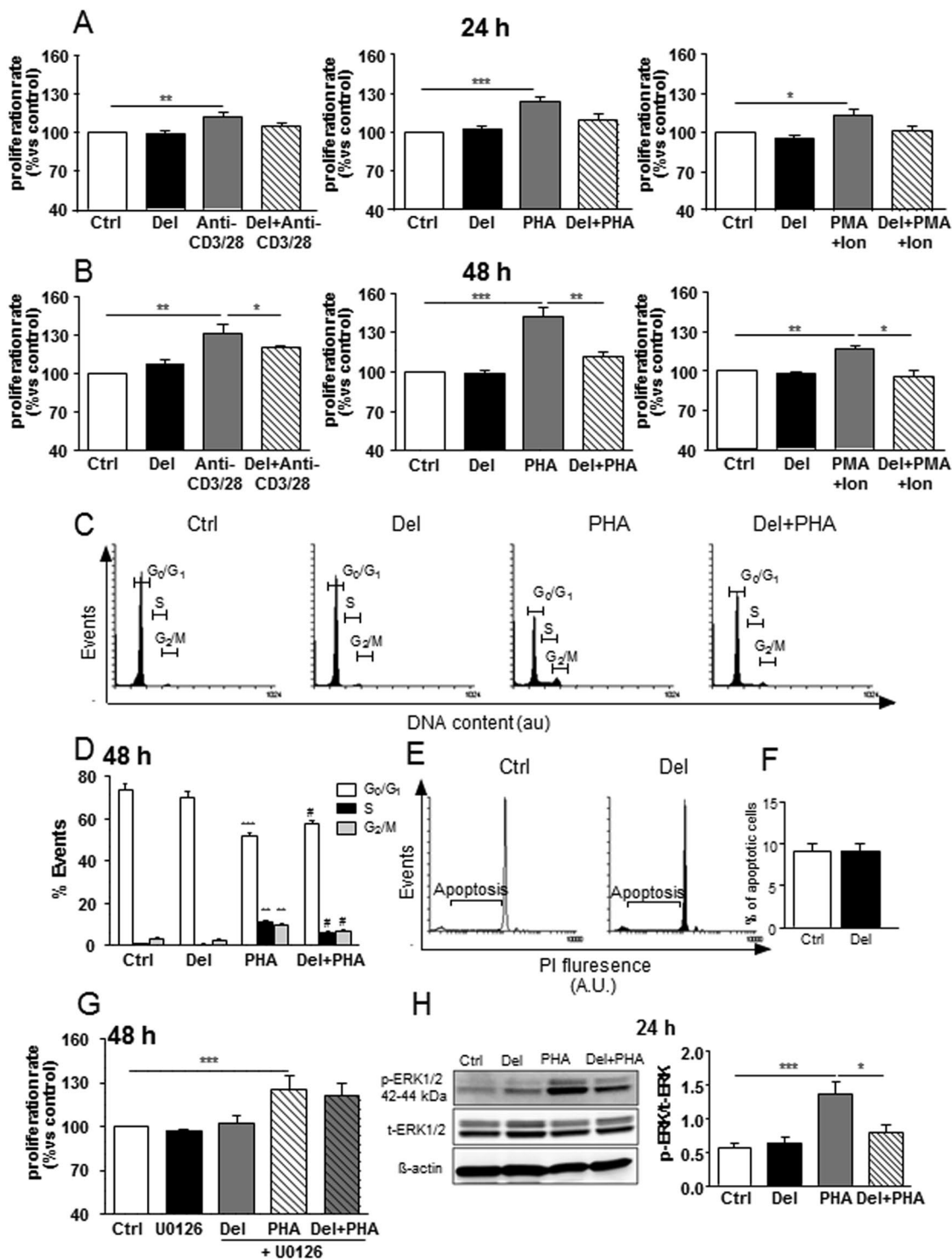


Figure 1. Effects of delphinidin on proliferation, cell cycle progression and ERK1/2 pathway activation of T lymphocytes from healthy subjects. Histograms show the percentage of proliferation of cells exposed to T cell activators [10 μ g/mL anti-CD3 plus 5 μ g/mL anti-CD28, 5 μ g/mL PHA or 10 ng/mL PMA plus 1 μ M ionomycin (Ion)] in absence or in presence of 10^{-2} g/L of delphinidin (Del) for 24 h (A) or 48 h (B). Data are the mean \pm SEM ($n = 5-10$). * $P < 0.05$, ** $P < 0.01$ and *** $P < 0.001$. (C) Representative cytometric profiles showing cells in the G₀/G₁, S and G₂/M phases of the cell cycle after 48 h of treatment with either 10^{-2} g/L of Del, 5 μ g/mL PHA or both. (D) Histograms show the percentage of the cells in the G₀/G₁, S and G₂/M phases determined by flow cytometric analysis. Data are the mean \pm SEM ($n = 12$). ** $P < 0.01$ and *** $P < 0.001$ versus control group. # $P < 0.05$ versus PHA group. (E) Representative histograms of flow cytometry showing sub-G1 peak, corresponding to the apoptotic population in propidium iodide (PI)-stained cells. (F) Quantification of sub-G1 peak. (G) Histograms show the percentage of proliferation of cells exposed to either 10^{-2} g/L of delphinidin (Del), 5 μ g/mL PHA or both in presence or in absence of 10 μ M of specific inhibitor

of ERK1/2 pathway (U0126) for 48 h. **(H)** Western blot of phosphorylated ERK1/2 in cells exposed to either 10^{-2} g/L of delphinidin (Del), 5 μ g/mL PHA or both during 24 h. Histograms show densitometric analysis of phosphorylated ERK1/2 normalized to total ERK1/2 expression. Data represent the mean \pm SEM ($n = 4-8$). * $P < 0.05$ and *** $P < 0.001$.

increase of $[Ca^{2+}]_i$ triggers different pathways including nuclear factor of activated T-cells (NFAT) and histone deacetylase (HDAC)⁸. These pathways mediate the functional modifications of T lymphocytes observed during chronic inflammation, including T cell proliferation and differentiation toward the pro-inflammatory cells over anti-inflammatory cells⁸⁻¹⁰.

Natural dietary polyphenolic compounds have been reported to protect against cardiovascular diseases and inflammation due to their multitude biological activities^{11, 12}. We have previously identified the anthocyanin, delphinidin, as a polyphenol with endothelium-dependent relaxation property by promoting nitric oxide (NO) production¹³. NO production induced by delphinidin involves activation of the isoform alpha of estrogen receptor (ER α)¹⁴ and increase of $[Ca^{2+}]_i$ ¹⁵. In addition, delphinidin inhibits endothelial cell proliferation by modulating the activity of MAP kinase^{16, 17}.

Given the crucial role of T lymphocytes in chronic inflammatory metabolic diseases, modulation of T lymphocytes function by using polyphenols as a possible approach might be of importance^{18, 19}. Jara *et al.*²⁰ have shown that delphinidin can activate NFAT and induce cytokine production through SOCE in T cells. In contrast, delphinidin suppresses NF- κ B acetylation and inhibits cytokine production in Jurkat cells²¹. However, the mechanism by which delphinidin affects T lymphocyte functions is not elucidated yet. Thus, the present study was carried out to analyze the effects of delphinidin on proliferation and differentiation of T lymphocytes isolated from healthy subjects and MetS patients. Further, we have examined the related signaling pathways involved in delphinidin effects.

Results

Delphinidin reduces the proliferation of T lymphocytes from healthy subjects. Delphinidin had no effect on basal proliferation of T cells treated for 24 or 48 h (Fig. 1A and B). Anti-CD3 plus anti-CD28 antibodies, PHA or PMA plus ionomycin significantly increased T cell proliferation after 24 and 48 h of treatment. Delphinidin prevented anti-CD3 plus anti-CD28-, PHA- and PMA plus ionomycin-induced proliferation of T lymphocytes at 48 h but not at 24 h (Fig. 1A and B). Thus, delphinidin has antiproliferative properties on T lymphocytes isolated from healthy subjects independent of the activated pathway. For the following experiments, the activator PHA has been chosen to study the mechanism by which delphinidin reduces T lymphocyte proliferation.

Delphinidin impairs cell cycle progression by inducing arrest in G₀/G₁ phase. The effect of delphinidin on cell cycle was evaluated at 48 h. Delphinidin had no effect on cell cycle compared to control cells. PHA alone induced a significant decrease of the cell population in G₀/G₁ phase, whereas the proportion of cells in S and G₂/M phases was increased in comparison to control cells (Fig. 1C and D). When T cells were treated with PHA and delphinidin, an increase of cells in G₀/G₁ phase, concomitant to a decrease of cells in S and G₂/M phases was observed when compared to PHA-treated T cells (Fig. 1C and D). Importantly, delphinidin had no effect on T cell apoptosis (Fig. 1E and F). Thus, the antiproliferative effect of delphinidin is associated with suppression of cell progression by blocking the cell cycle in G₀/G₁ phase.

Delphinidin inhibits T lymphocyte proliferation through ERK1/2 kinase-dependent pathway. The potential implication of ERK1/2 in the antiproliferative effect of delphinidin was tested using a specific ERK1/2 pathway inhibitor (U0126)^{6, 22-24}. U0126 alone did not affect the proliferation of T cells isolated from healthy subjects (Fig. 1G). Noticeably, in the presence of U0126, delphinidin failed to reduce proliferation induced by PHA (Fig. 1G).

To confirm these results, ERK1/2 activation was assessed by Western blot after 10, 30 min, 1, 24 and 48 h of T cells treated with PHA, delphinidin or both. As shown in Supplementary Fig. 1, an increase of ERK1/2 phosphorylation was observed at 10 min and maintained even after 30 min, or 24 h following PHA stimulation. Delphinidin had no effect on basal ERK1/2 activity at any time points, but it prevented the PHA-induced ERK1/2 activation after 24 h of PHA stimulation (Fig. 1H). Altogether, these results suggest that delphinidin inhibits T lymphocyte proliferation through ERK1/2 kinase-dependent pathway. Moreover, they support the hypothesis that ERK1/2 occurred at the early event leading to cell proliferation.

Delphinidin inhibits T lymphocyte proliferation through SOCE-dependent pathway. T lymphocyte activation induces an augmentation of $[Ca^{2+}]_i$ principally by SOCE, which is an essential step in their proliferation^{25, 26}. The SOCE inhibitor, SKF96365, had no effect on T cell proliferation, but it prevented the PHA-induced proliferation after 48 h of treatment (Fig. 2A). Delphinidin failed to reduce further T cell proliferation in presence of PHA plus SKF96365 (Fig. 2A). Then, the effect of delphinidin was investigated on Ca^{2+} signaling. Delphinidin had no effect on basal $[Ca^{2+}]_i$ but it significantly decreased the thapsigargin-induced $[Ca^{2+}]_i$ increase in Ca^{2+} -containing PSS (Fig. 2B). SKF96365 reduced the increase of $[Ca^{2+}]_i$ induced by thapsigargin. Interestingly, the effect of delphinidin on the thapsigargin-induced $[Ca^{2+}]_i$ increase was completely abrogated in presence of SKF96365 (Fig. 2C).

In order to investigate the source of Ca^{2+} implicated in the activation of T lymphocytes, the effects of delphinidin on $[Ca^{2+}]_i$ increase induced by $CaCl_2$ addition after depletion of intracellular stores by thapsigargin in

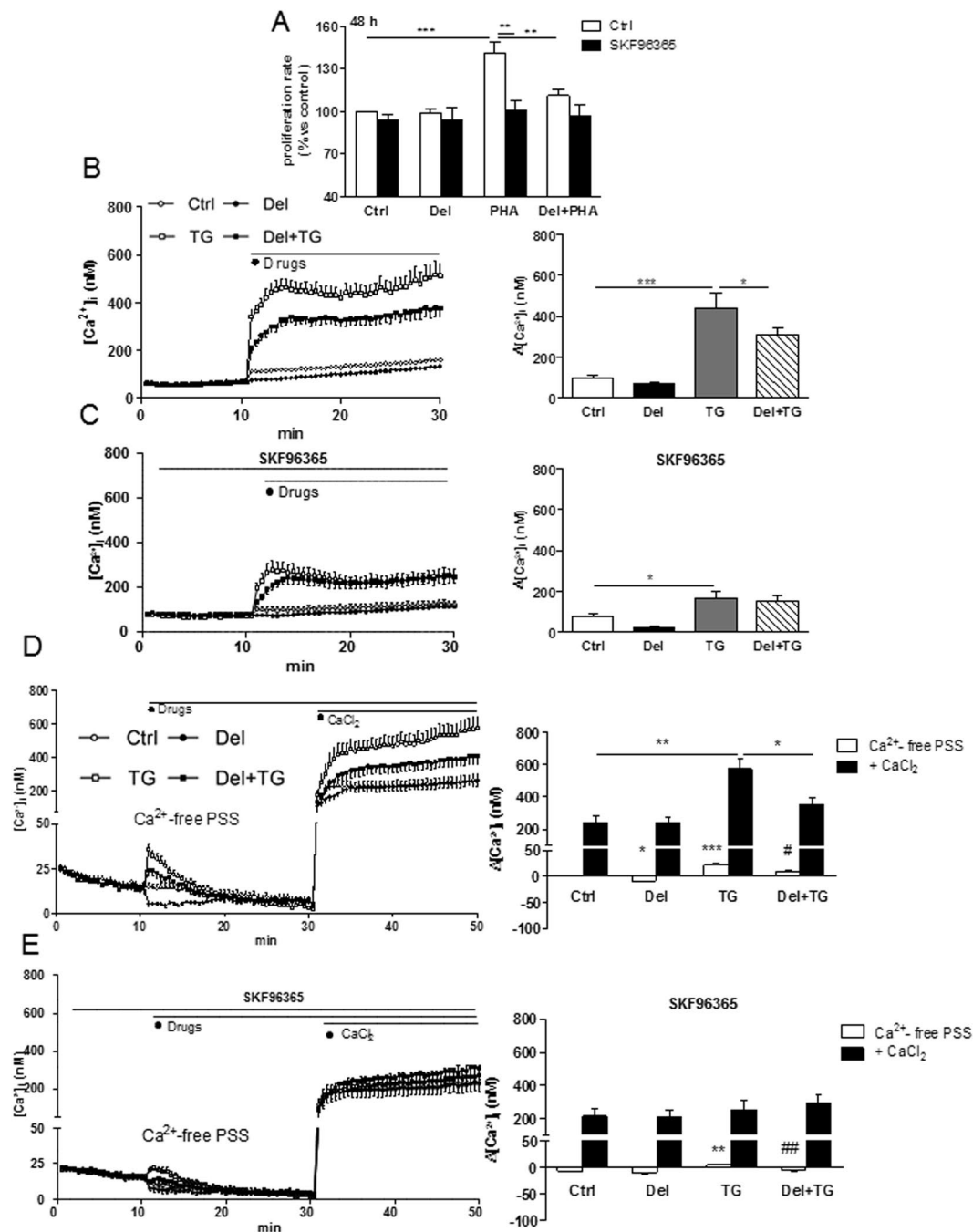


Figure 2. Delphinidin inhibits T lymphocyte proliferation through SOCE-dependent pathway. (A) Histograms show the percentage of proliferation of cells exposed to either 10^{-2} g/L of delphinidin (Del), $5 \mu\text{g/mL}$ PHA or both, in absence or in presence of $10 \mu\text{M}$ of SOCE inhibitor (SKF96365) for 48 h. (B) Representative traces (left) and histograms (right) showing the effect of 10^{-2} g/L of delphinidin (Del) alone or after activation by $1 \mu\text{M}$ thapsigargin (TG) on $[Ca^{2+}]_i$ in Ca^{2+} -containing PSS. (C) Same experiments in presence of $10 \mu\text{M}$ of SOCE inhibitor (SKF96365). (D) Representative traces (left) and histograms (right) showing the effect of 10^{-2} g/L delphinidin on $[Ca^{2+}]_i$ increase induced by 1.25 mM of $CaCl_2$ after depletion of intracellular stores in Ca^{2+} -free PSS by $1 \mu\text{M}$ TG. (E) Same experiments in presence of $10 \mu\text{M}$ of SOCE inhibitor, SKF96365. Data are the mean \pm SEM ($n = 7-11$). * $P < 0.05$, ** $P < 0.01$ and *** $P < 0.001$ versus control group. # $P < 0.05$ and ## $P < 0.01$ versus TG group.

Ca^{2+} -free solution was investigated. Delphinidin reduced basal $[Ca^{2+}]_i$ in Ca^{2+} -free PSS. Moreover, delphinidin reduced both the thapsigargin-induced $[Ca^{2+}]_i$ increase resulting from the release of Ca^{2+} from intracellular stores and the Ca^{2+} influx from extracellular medium after $CaCl_2$ addition (Fig. 2D). The effect of delphinidin on thapsigargin-induced $[Ca^{2+}]_i$ increase resulting from the influx of extracellular Ca^{2+} was completely abolished in

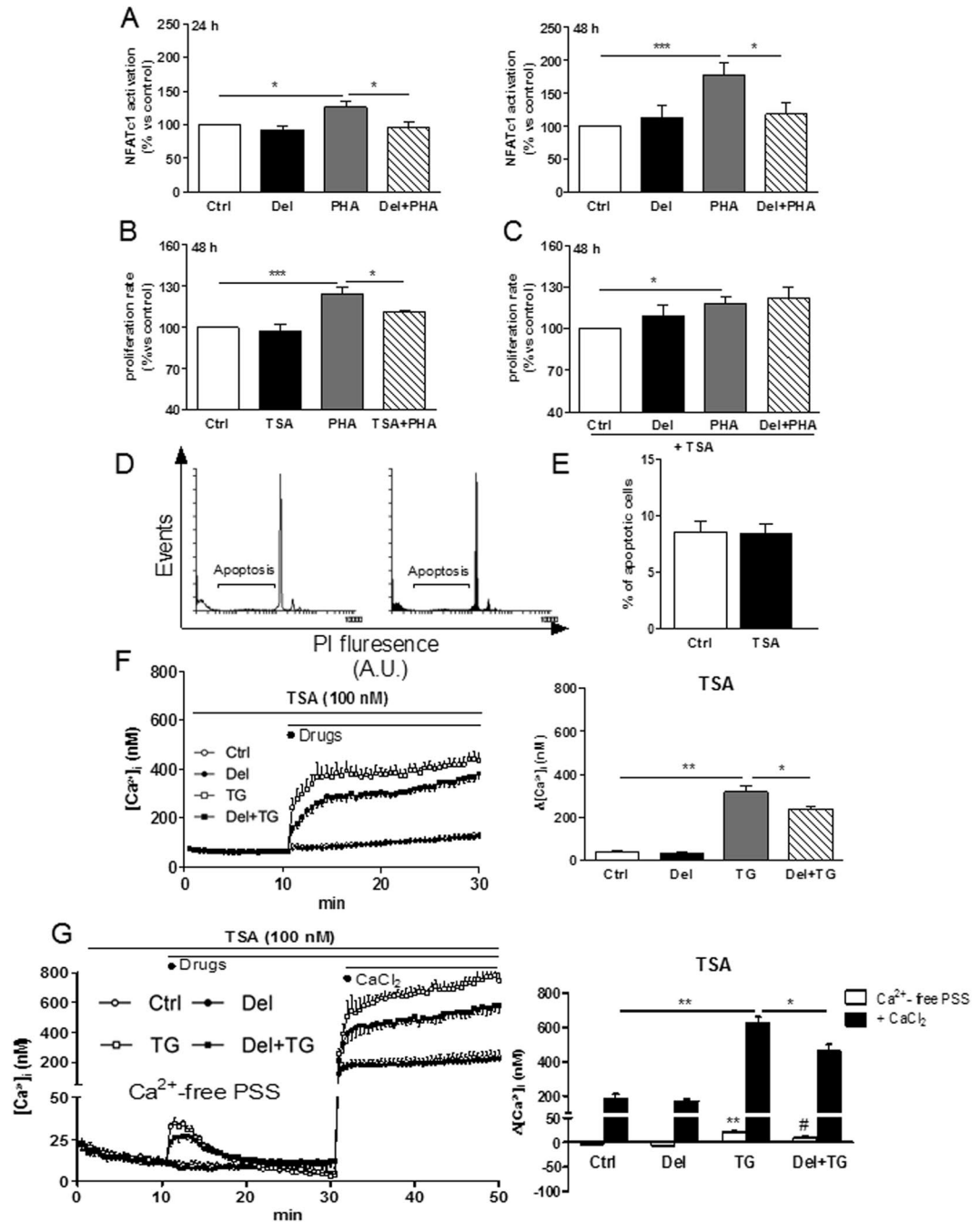


Figure 3. Delphinidin inhibits T lymphocyte proliferation through NFAT and HDAC-dependent pathway. (A) Histograms show the percentage of NFAT activation of cells exposed to either 10^{-2} g/L of delphinidin (Del), 5 μ g/mL PHA or both for 24 and 48 h. (B) Histograms show the percentage of proliferation of cells exposed to HDAC inhibitor (TSA, 100 nM), 5 μ g/mL PHA or both for 48 h. (C) Histograms show the percentage of proliferation of cells exposed to either 10^{-2} g/L of delphinidin (Del), 5 μ g/mL PHA or both in presence of 100 nM of TSA for 48 h. Data are the mean \pm SEM ($n = 5$). * $P < 0.05$ and *** $P < 0.001$. (D) Representative histograms of flow cytometry showing sub-G1 peak, corresponding to the apoptotic population in propidium iodide (PI)-stained cells. (E) Quantification of sub-G1 peak. (F) Representative traces (left) and histograms (right) showing the effect of 10^{-2} g/L of delphinidin (Del) alone or after activation by 1 μ M thapsigargin (TG) on $[Ca^{2+}]_i$ in Ca^{2+} -containing PSS in presence of 100 nM of TSA. (G) Representative traces (left) and histograms (right) showing the effect of 10^{-2} g/L delphinidin on $[Ca^{2+}]_i$ increase induced by 1.25 mM of $CaCl_2$ after depletion of intracellular stores in Ca^{2+} -free PSS by 1 μ M TG in presence of 100 nM of TSA. Data are the mean \pm SEM ($n = 5-8$). * $P < 0.05$ and ** $P < 0.01$. *** $P < 0.01$ versus control group, * $P < 0.05$ versus TG group.

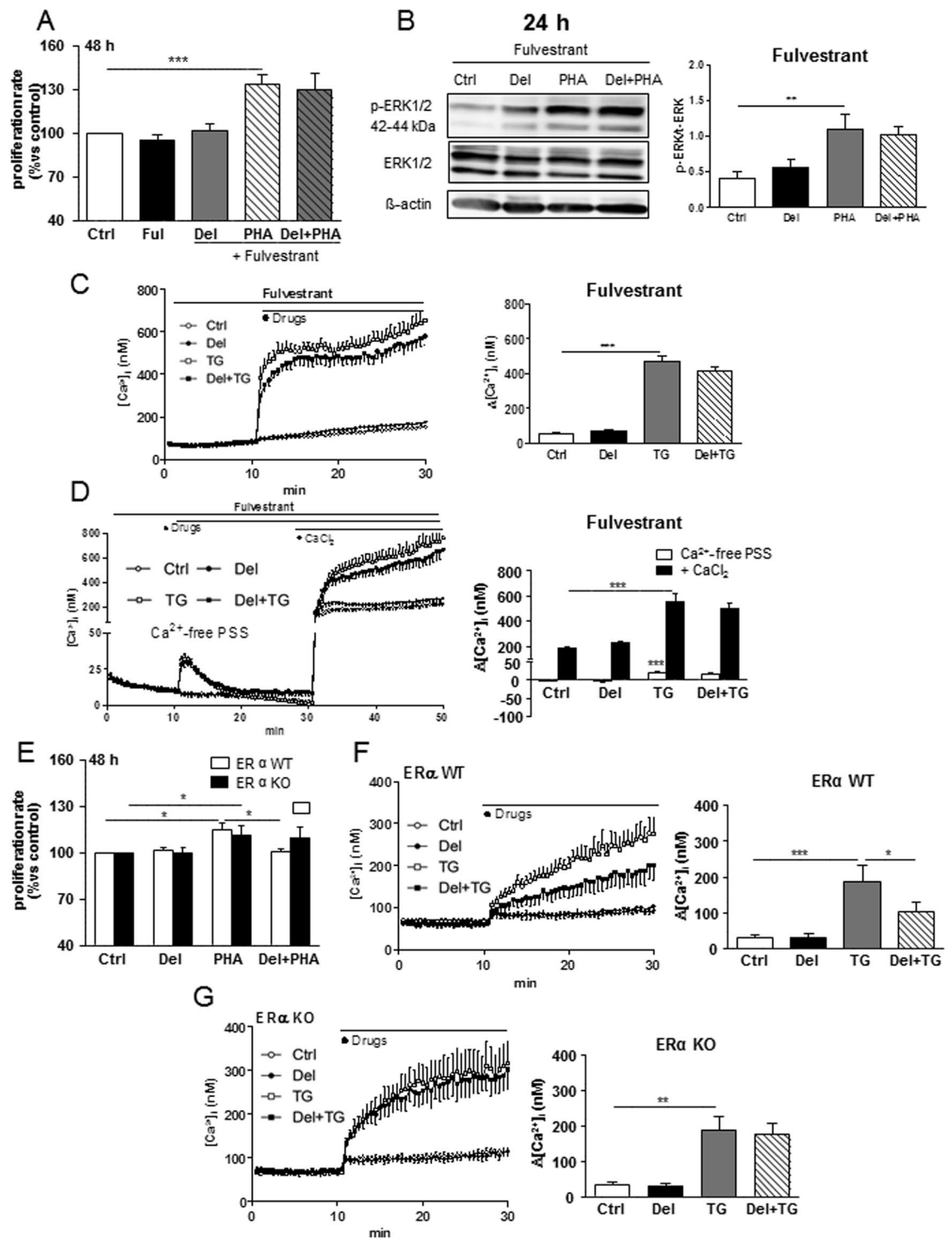


Figure 4. Delphinidin inhibits T lymphocyte proliferation through ER α -dependent mechanism. (A) Histograms show the percentage of proliferation of cells exposed to either 10^{-2} g/L of delphinidin (Del), 5 μ g/mL PHA or both in presence or in absence of nonselective estrogen receptor antagonist (Fulvestrant 100 nM) for 48 h. Data are the mean \pm SEM ($n = 8$). (B) Western blot of phosphorylated ERK1/2 in T cells exposed to either 10^{-2} g/L of delphinidin, 5 μ g/mL PHA or both for 24 h in presence of fulvestrant. Histograms show densitometric analysis of phosphorylated ERK1/2 normalized to total ERK1/2 expression, Data are the mean \pm SEM ($n = 6$). (C) Representative traces (left) and histograms (right) showing the effect of 10^{-2} g/L of delphinidin alone or after activation by 1 μ M thapsigargin (TG) on [Ca²⁺]_i in Ca²⁺-containing PSS in presence of Ful (100 nM). (D) Representative traces (left) and histograms (right) showing the effect of delphinidin on [Ca²⁺]_i increase induced by 1.25 mM of CaCl₂ after depletion of intracellular stores in Ca²⁺-free PSS by thapsigargin in presence of fulvestrant. Data are the mean \pm SEM ($n = 7$). (E) Histograms show the percentage of proliferation of cells isolated from ER α WT or KO mice exposed to either 10^{-2} g/L of delphinidin, 5 μ g/mL

PHA or both for 48 h. **(F)** Representative traces (*left*) and histograms (*right*) showing the effect of 10^{-2} g/L of delphinidin (Del) alone or after activation by $1 \mu\text{M}$ thapsigargin (TG) on $[\text{Ca}^{2+}]_i$ in Ca^{2+} -containing PSS of cells isolated from ER α WT mice. **(G)** Same experiments on cells isolated from ER α KO mice. Data are the mean \pm SEM ($n = 4$). * $P < 0.05$, ** $P < 0.01$ and *** $P < 0.001$ versus control group.

presence of SKF96365 (Fig. 2E). Altogether, these data highlight that the antiproliferative effect of delphinidin is associated with its ability to inhibit Ca^{2+} influx through SOCE.

Delphinidin inhibits T lymphocyte proliferation through NFAT-dependent pathway. The implication of NFAT pathway in the antiproliferative effect of delphinidin was investigated. Delphinidin alone had no effect on NFAT activation compared to control cells (Fig. 3A). Interestingly, delphinidin decreased the PHA-induced NFAT activation at 24 and 48 h demonstrating that the antiproliferative effect of delphinidin is associated with its ability to inhibit NFAT activation (Fig. 3A).

Delphinidin inhibits T lymphocyte proliferation through HDAC-dependent pathway. The role of HDAC in the antiproliferative properties of delphinidin was investigated using the HDAC inhibitor (TSA). TSA did not modify the basal proliferation of T cells but it was able to inhibit the PHA-induced proliferation (Fig. 3B). Furthermore, at 48 h, the antiproliferative effect of delphinidin was completely prevented in presence of TSA (Fig. 3C). The concentration of TSA used in this study did not induce apoptosis (Fig. 3D and E). Thus, delphinidin prevents the proliferation of T lymphocytes by a mechanism sensitive to inhibition of HDAC activity.

The role of Ca^{2+} signaling in the HDAC-dependent antiproliferative effect of delphinidin was analyzed. TSA had no effect on the basal $[\text{Ca}^{2+}]_i$ nor on the thapsigargin-induced $[\text{Ca}^{2+}]_i$ increase in both Ca^{2+} -containing and Ca^{2+} -free PSS (Supplementary Fig. 2). Interestingly, delphinidin was still able to reduce the ability of thapsigargin to increase $[\text{Ca}^{2+}]_i$ in the presence of TSA (Fig. 3F and G). These results suggest that delphinidin inhibits HDAC activity by a mechanism downstream of its effect on Ca^{2+} signaling.

Delphinidin inhibits T lymphocyte proliferation through ER α -dependent mechanism. Next, we investigated the implication of ER α in controlling the antiproliferative properties of delphinidin. The ER antagonist, fulvestrant, at a concentration at which it had no effect by itself on T cell proliferation, abolished the antiproliferative effect of delphinidin (Fig. 4A). Interestingly, fulvestrant also prevented the ability of delphinidin to decrease the PHA-induced ERK1/2 phosphorylation (Fig. 4B). Moreover, fulvestrant prevented the ability of delphinidin to inhibit the increase of $[\text{Ca}^{2+}]_i$ induced by thapsigargin both in Ca^{2+} -containing and Ca^{2+} -free PSS (Fig. 4C and D).

To further characterize the ER isoform involved in delphinidin effects, the same experimental protocols were conducted in peripheral blood mononuclear cells (PBMCs) isolated either from ER α WT or KO mice. Interestingly, delphinidin prevented the PHA-induced proliferation in PBMCs isolated from WT but not from KO mice (Fig. 4E). In addition, delphinidin decreased the thapsigargin-induced $[\text{Ca}^{2+}]_i$ increase in T cells isolated from WT but not from KO mice (Fig. 4F and G). Altogether, these results demonstrate that delphinidin exerts its antiproliferative effect resulting from inhibition of Ca^{2+} entry and ERK1/2 activation via the α isoform of the ER.

Delphinidin decreases Th1, Th17, Treg but not Th2 differentiation of T lymphocytes from healthy subjects. The effect of delphinidin on the differentiation of T lymphocytes from healthy subjects following 24 h of PHA treatment was analyzed. As shown in Fig. 5A and Supplementary Fig. 3, PHA increased the expression of T-bet, GATA3, ROR γ t and FOXP3 (the transcription factors that control Th1, Th2, Th17 and Treg, respectively) compared to control cells. Delphinidin had no effect on basal expression of these factors but it was able to decrease the PHA-induced T-bet, ROR γ t and FOXP3 but not GATA3 expression.

To confirm these results, we investigated the production of IFN γ , IL-4, IL-17A, IL-10 (produced by Th1, Th2, Th17 and Treg, respectively), and IL-2, following delphinidin treatment in activated T cells. In order to get a high production of cytokines over a short time, T lymphocytes were stimulated by PMA plus ionomycin during 5 h. T cells treated with PMA plus ionomycin displayed an increase in IL-2, IFN γ , IL-4, IL-17A and IL-10 production (Fig. 5B, Supplementary Fig. 4). Delphinidin did not modify basal production of any cytokines, whereas it reduced the increase of IL-2, IFN γ , IL-17A, IL-10 but not IL-4 production induced by PMA plus ionomycin. These results suggest that delphinidin inhibits T cell differentiation toward Th1, Th17, Treg but not Th2 subsets.

Delphinidin reduces proliferation and Ca^{2+} signaling in T lymphocytes from patients with cardiovascular risk factors displaying one or two criteria of MetS. Immuno-modulatory and anti-inflammatory properties of delphinidin in T lymphocytes from healthy subjects highlighted the potential of this polyphenol to modulate chronic inflammation associated with metabolic diseases. To confirm this hypothesis, the effects of delphinidin on proliferation and Ca^{2+} signaling of T lymphocytes from non-MetS and MetS patients were studied. Delphinidin did not modify the basal proliferation of T lymphocytes from non-MetS and MetS patients. Delphinidin displayed antiproliferative effects on T lymphocytes from non-MetS patients but not those from MetS patients treated for 48 h with PHA (Fig. 6A and B).

Delphinidin did not alter basal $[\text{Ca}^{2+}]_i$ in T cells from non-MetS patients, but it decreased the thapsigargin-induced $[\text{Ca}^{2+}]_i$ increase in Ca^{2+} -containing PSS (Fig. 6C). Furthermore, delphinidin reduced the thapsigargin-induced $[\text{Ca}^{2+}]_i$ increase resulting from Ca^{2+} release and Ca^{2+} influx after CaCl_2 addition (Fig. 6D). Conversely, delphinidin did not alter the basal $[\text{Ca}^{2+}]_i$ nor the thapsigargin-induced $[\text{Ca}^{2+}]_i$ increase (Fig. 6E and F) in T cells from MetS patients.

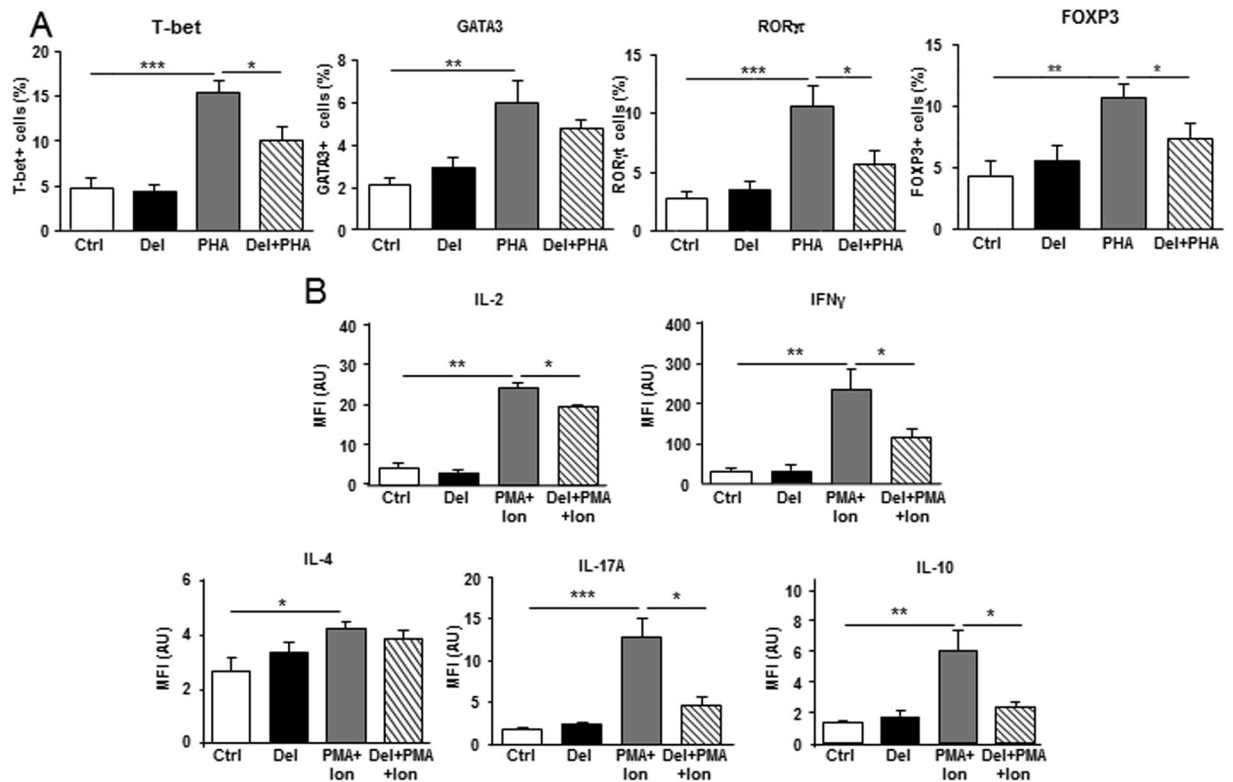


Figure 5. Effect of delphinidin on the differentiation of T lymphocytes from healthy subjects. (A) Cells were stimulated for 24 h with 10^{-2} g/L of delphinidin (Del), 5 μ g/mL of PHA or both and stained for T-bet, GATA3, ROR γ t and FOXP3 transcription factors. Histograms show the percentage of positive cells for T-bet, GATA3, ROR γ t and FOXP3 expressions. Data are the mean \pm SEM ($n = 7$). (B) T cells were stimulated for 5 h with 10^{-2} g/L of delphinidin (Del), 50 ng/mL phorbol-12-myristate-13-acetate (PMA) plus 1 μ g/mL ionomycin (Ion) or both, in the presence of 5 μ g/mL brefeldin A (BFA) for the last 3 h of culture and stained for IL-2, IFN γ , IL-4, IL-17A and IL-10 cytokines. Histograms show the MFI of positive cells for IL-2, IFN γ , IL-4, IL-17A, and IL-10, respectively. Data are the mean \pm SEM ($n = 7$). * $P < 0.05$, ** $P < 0.01$ and *** $P < 0.001$.

Altogether, these results highlight the potential of delphinidin to reduce proliferation and Ca²⁺ signaling in T lymphocytes isolated from patients with cardiovascular risk factors displaying one or two criteria of MetS. Accordingly, a negative correlation between the number of MetS criteria and the inhibition of proliferation by delphinidin has been observed (Fig. 6G).

Delphinidin decreases Th17 and Treg differentiation of T lymphocytes from patients with cardiovascular risk factors displaying one or two criteria of MetS. The effect of delphinidin on the differentiation of T lymphocytes from non-MetS and MetS patients following 24 h of PHA treatment was further investigated. Delphinidin alone had no effects on T-bet, GATA3, ROR γ t and FOXP3 expression (data not shown). Alternatively, delphinidin reduced the PHA-induced ROR γ t and FOXP3 expression in T cells from non-MetS patients, while it had no effects on T cells from MetS patients (Fig. 7A). PHA-induced-T-bet and GATA3 expression of T cells from both non-MetS and MetS patients were unchanged by delphinidin (Fig. 7A).

To further confirm these results, the secretion of IL-2, IFN γ , IL-4, IL-17 and IL-10 in the corresponding cellular supernatants was assessed. PHA increased all cytokines of T cells from non-MetS and MetS patients (Fig. 7B). Delphinidin did not modify basal production of any cytokines (data not shown). Interestingly, it reduced the PHA-stimulated secretion of pro-inflammatory cytokine IL-2, whatever the source of T cells (Fig. 7C). Alternatively, delphinidin decreased IL-17A and IL-10 secretion only in non-MetS patients-derived T cells treated with PHA. PHA-induced IFN γ and IL-4 secretion were unmodified by delphinidin in both T cell types (Fig. 7C). Therefore, modulation of cytokines secretion by T lymphocytes in response to delphinidin was influenced by the number of cardiovascular risk factors, as illustrated by the negative correlation found between the number of MetS criteria and the inhibition of IL-17 secretion by delphinidin (Fig. 7D). Altogether, these results suggest that delphinidin inhibits T cell differentiation toward Th17 and Treg subsets of T lymphocytes from patients with cardiovascular risks displaying one or two criteria of MetS.

Discussion

The present study shows that delphinidin inhibits proliferation of T lymphocytes from healthy subjects and patients with cardiovascular risk factors displaying one or two criteria of MetS by preventing the progression into S and G₂/M phases of the cell cycle. The antiproliferative effect of delphinidin is related to its capacity to inhibit

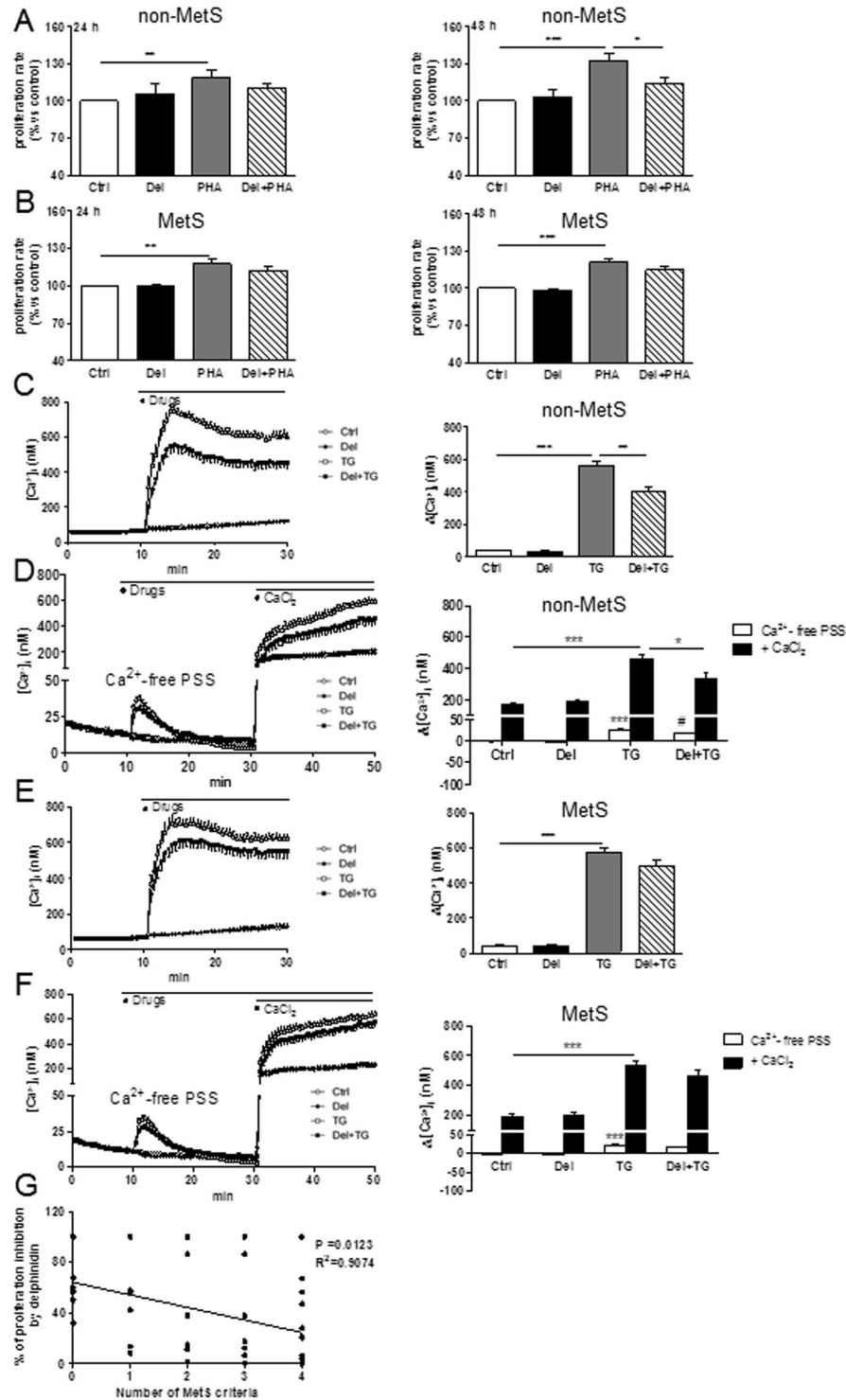


Figure 6. Effects of delphinidin on proliferation and Ca²⁺ signaling of T lymphocytes from non-MetS and MetS patients. **(A)** Histograms show the percentage of proliferation of cells isolated from non-MetS patients exposed to either 10⁻² g/L of delphinidin (Del), 5 μg/mL PHA or both for 24 and 48 h. **(B)** Same experiments on cells isolated from MetS patients. Data are the mean ± SEM (n = 8–31). **(C)** Representative traces (left) and histograms (right) showing the mean of the responses induced by 10⁻² g/L of delphinidin (Del) alone or after activation by 1 μM thapsigargin (TG) on [Ca²⁺]_i in Ca²⁺-containing PSS of T cells isolated from non-MetS patients. **(D)** Representative traces (left) and histogram (right) showing the effect of 10⁻² g/L Del on [Ca²⁺]_i increase induced by 1.25 mM of CaCl₂ after depletion of intracellular stores in Ca²⁺-free PSS by 1 μM TG of cells isolated from non-MetS patients. Data are the mean ± SEM (n = 12–14). **(E and F)** Same experiments as (C and D, respectively) on cells isolated from MetS patients. **(G)** Negative correlation between Del effect on PHA-induced proliferation and number of MetS criteria. Data are the mean ± SEM (n = 16). *P < 0.05, **P < 0.01 and ***P < 0.001. ***P < 0.001 versus control group, #P < 0.05 versus TG group.

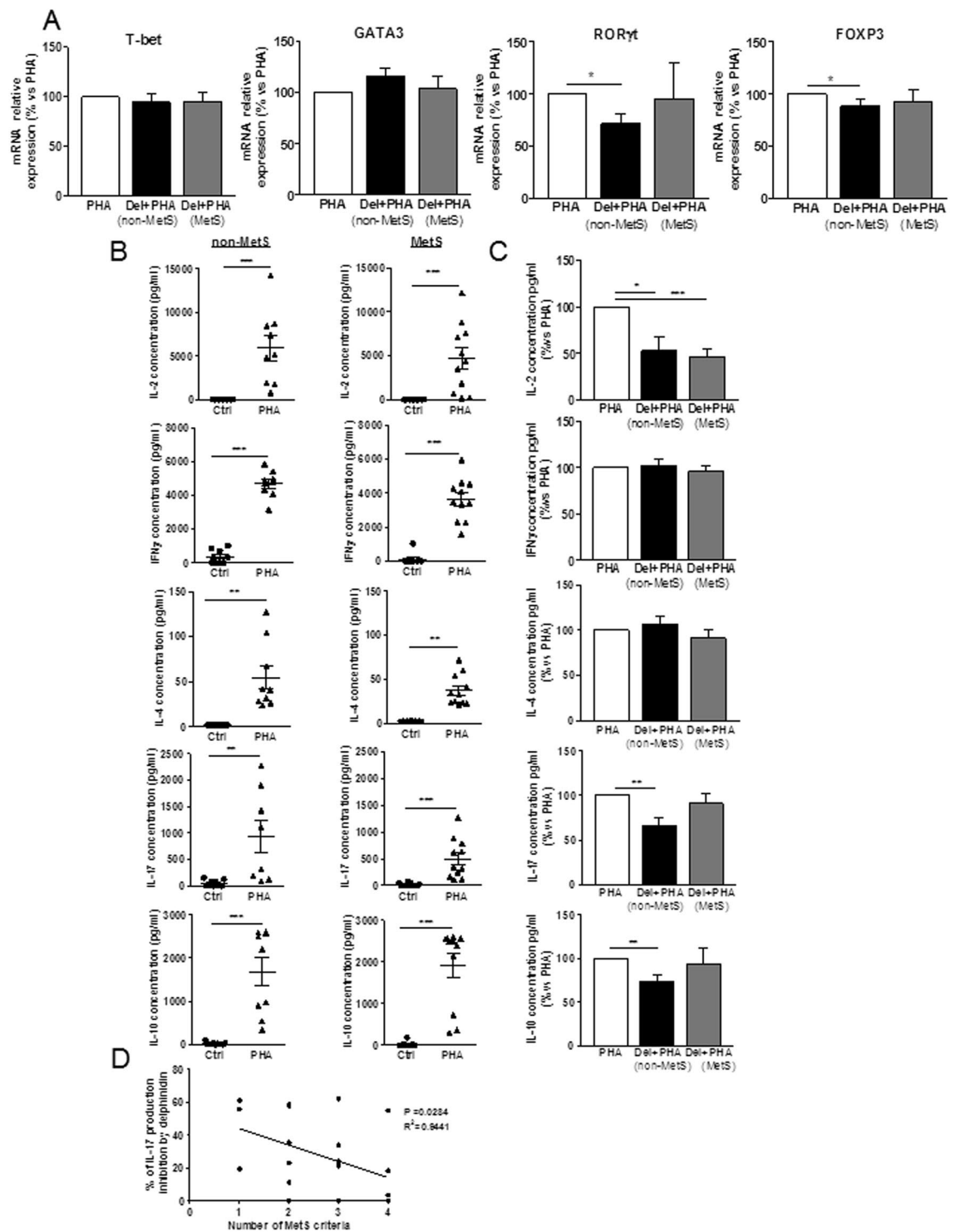


Figure 7. Effect of delphinidin on the differentiation of T lymphocytes from non-MetS and MetS patients. Cells isolated from non-MetS (1–2 criteria) and MetS (3, 4 or 5 criteria) patients were stimulated for 24 h with 10^{-2} g/L of delphinidin (Del), 5 μ g/mL of PHA or both. **(A)** The expression of T-bet, GATA3, ROR γ t and FOXP3 transcription factors in treated cells was measured by RT-qPCR. Results are normalized with the gene reference and expressed as relative expression compared to PHA group. Data are the mean \pm SEM ($n = 5$ –10). The production of IL-2, IFN γ , IL-4, IL-17 and IL-10 was measured in supernatants of treated cells using Magnetic Luminex Screening Assay. **(B)** Effects of PHA on cytokine production compared to controls cells. **(C)** The effect of delphinidin on cytokines production induced by PHA in non-MetS and MetS-derived cells. Data are the mean \pm SEM ($n = 9$ –11). **(D)** Negative correlation between delphinidin effect on PHA-induced IL-17 production and number of MetS criteria. * $P < 0.05$, ** $P < 0.01$ and *** $P < 0.001$.

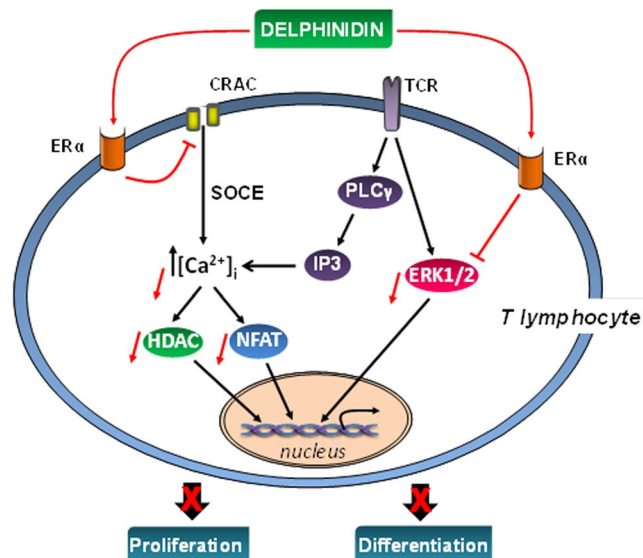


Figure 8. Summary of the mechanisms of the biological effects of delphinidin on T lymphocytes. Delphinidin inhibits ERK1/2, NFAT and HDAC pathways activation, also it decreases $[Ca^{2+}]_i$ augmentation by inhibiting intracellular Ca^{2+} release and extracellular Ca^{2+} entry through CRAC channels. These effects occur mostly via $ER\alpha$ -dependent mechanism resulting in inhibition of proliferation and differentiation of T lymphocytes.

ERK1/2, NFAT and HDAC pathways. Interestingly, delphinidin decreases $[Ca^{2+}]_i$ signaling by inhibiting intracellular Ca^{2+} release and extracellular Ca^{2+} entry through CRAC channels. In addition, delphinidin inhibits the differentiation of T lymphocytes from healthy subjects toward Th1, Th17, Treg but not Th2 subsets. The inhibitory effects of delphinidin on Th17 and Treg differentiation are moreover conserved in T cells from patients with cardiovascular risk factors. The present study identifies $ER\alpha$ as the key receptor mediating the immunomodulatory effect of delphinidin (Fig. 8).

Abnormal T lymphocyte activation is one of the major causes of chronic inflammation-associated diseases^{27, 28}. Since obesity-related metabolic diseases are associated with an increase in T lymphocyte proliferation⁴, inhibition of T cell proliferation has been reported to have beneficial effects against such diseases^{5, 29–32}. We reported that delphinidin inhibited the proliferation of T lymphocytes from healthy subjects stimulated by different agents such as anti-CD3 plus anti-CD28, PHA or PMA plus ionomycin. Thus, delphinidin may have beneficial effects in treating chronic inflammatory metabolic diseases by inhibiting T lymphocyte proliferation.

Cell cycle analysis showed that delphinidin inhibited progression into S and G_2/M phases of cell cycle of T cells. Consequently, the cells accumulate in G_0/G_1 phase. Since delphinidin treatment did not induce apoptosis, the observed accumulation in G_0/G_1 phase reflected a specific effect of delphinidin on cell cycle progression rather than a decrease of cell number due to apoptosis. These observations are in agreement with our former data showing that delphinidin impairs cell cycle progression of endothelial cells through blocking G_1/S transition¹⁷.

TCR activation triggers several pathway implicated in T cell proliferation, including ERK1/2⁶. Blocking ERK1/2 activation has been identified as one of the mechanisms by which anthocyanins, including delphinidin, exert their antiproliferative activity towards multiple cancer cell types^{33–35}. The antiproliferative effect of delphinidin was abolished in presence of ERK1/2 pathway inhibitor, U0126. Furthermore, delphinidin was able to decrease the PHA-induced ERK1/2 activation after 24 h of treatment. Thus, it acts at the early event of T cell proliferation observed at 48 h.

$[Ca^{2+}]_i$ increase plays an important role in T lymphocyte proliferation²⁵. Herein, delphinidin inhibited $[Ca^{2+}]_i$ increase induced by thapsigargin, used to mimic TCR stimulation via an increase in $[Ca^{2+}]_i$ resulting from Ca^{2+} release from internal source followed by SOCE. Interestingly, the effect of delphinidin on the thapsigargin-induced $[Ca^{2+}]_i$ increase was completely abrogated in presence of SKF96365. In addition, the antiproliferative effect of delphinidin was abolished in presence of SKF96365. It should be noted that the pharmacological inhibitor of voltage-dependent Ca^{2+} channel, mibefradil, used at maximally active concentration of 3 μM , did not affect the response to thapsigargin (Supplementary Fig. 5). Moreover, delphinidin was able to reduce Ca^{2+} signaling induced by thapsigargin in the presence of this inhibitor (Supplementary Fig. 5), demonstrating that voltage-operated Ca^{2+} channels were not involved neither in the response to thapsigargin nor the inhibitory effect of delphinidin, under the experimental condition used. Altogether, it can be hypothesized that delphinidin reduces T cell proliferation most likely via inhibition of Ca^{2+} entry via SOCE.

$[Ca^{2+}]_i$ increase triggers NFAT pathway that controls T lymphocyte proliferation^{36, 37}. Delphinidin decreased the PHA-induced NFAT activity after 24 and 48 h. These results suggest that inhibiting TCR- Ca^{2+} -NFAT axis is one of the mechanisms by which delphinidin exerts its antiproliferative properties on T cells.

Histone acetylation–deacetylation is an important Ca^{2+} -dependent epigenetic event that control T cell proliferation^{38, 39}. HDAC inhibitors decrease T cell proliferation without affecting $[Ca^{2+}]_i$ ^{40, 41}. In agreement with these findings, TSA decreased the PHA-induced proliferation without affecting Ca^{2+} signaling in T cells. Furthermore,

the antiproliferative effect of delphinidin was abolished in presence of TSA. Altogether, our results suggest that modulating HDAC activity might be an additional mechanism by which delphinidin exerts its antiproliferative effect on T cells. In line with these results, delphinidin has been shown to modulate the balance between HDAC and histone acetyltransferase (HAT) by inhibiting HAT activity in MH7A cells²¹. Delphinidin ability to decrease $[Ca^{2+}]_i$ was not modified in presence of TSA suggesting that its effect on HDAC is downstream of $[Ca^{2+}]_i$ signaling.

The present study identified ER α as the key receptor transducing antiproliferative effect exerted by delphinidin on T lymphocytes. Indeed, we show that the antiproliferative properties of delphinidin, as well as its effects on Ca^{2+} signaling and ERK1/2 pathway, were abolished after pharmacological blockade of ER with fulvestrant. Most importantly, deletion of ER α completely abolished the effects of delphinidin on proliferation and Ca^{2+} signaling of murine PBMCs. These results are in agreement with previous study in which ER α has been identified to mediate delphinidin beneficial effects on endothelial cells¹⁴. We provide further evidence of ER α as a target of delphinidin on T lymphocytes.

Interestingly, delphinidin decreased the PHA-induced proliferation and the thapsigargin-induced $[Ca^{2+}]_i$ increase in T cells from patients with cardiovascular risk factors but not from MetS patients. A negative correlation was found between delphinidin capacity to decrease the PHA-induced proliferation and the number of MetS criteria. This differential effect might be explained by alterations of ER α expression on T lymphocytes from MetS patients compared to healthy subjects and non-MetS patients. Indeed, the expression of ER α is lower in T cells of patients with chronic inflammatory diseases like systemic lupus erythematosus, which is characterized by wide-spread inflammation with high pro-inflammatory cytokines^{42,43}. Similarly, ER α expression is decreased in splenocytes of animals subjected to trauma and hemorrhage, a general inflammatory condition, compared to control animals⁴⁴. In addition, others studies have reported a decreased inflammation-associated ER α expression in other cell types^{45–47}. These studies support a concept of down-regulation of ER α under inflammatory conditions, which might lead to a reduced signaling through ER α pathways.

In addition to T cell proliferation increase, diet-related metabolic disorders are associated with increased T lymphocyte differentiation toward pro-inflammatory subsets with relative decline in anti-inflammatory subsets⁴⁸. Delphinidin decreased the differentiation of T cells from healthy subjects toward Th1, Th17, Treg but not Th2 subsets. Indeed, delphinidin treatment decreased the expression of Th1, Th17 and Treg subsets-specific transcription factors as well as the cytokines produced by these respective T subsets. Interestingly, delphinidin had no effect on Th2-specific transcription factor or Th2-signature cytokine. This might be due to the difference in IP₃ and Ca^{2+} signaling in Th2 cells compared to other CD4⁺ subsets. Indeed, TCR activation is not able to increase IP₃ and $[Ca^{2+}]_i$ in Th2 cells⁴⁹. Furthermore, the inhibitory effects of delphinidin on Th17 and Treg differentiation were moreover conserved in T cells isolated from patients with cardiovascular risk factors. It is noteworthy that delphinidin effect on IL-17 production is negatively correlated with the number of MetS criteria.

Delphinidin was able to decrease the production of pro-inflammatory cytokine IL-2 in T cells from non-MetS and MetS patients. NFAT can act with multiple transcriptional partners (AP-1, NfK-B, STAT3, STAT5, Smad2/3) and targets (IL-2, T-bet, GATA3, ROR γ t and FOXP3)⁵⁰. In the present study, NFAT signaling participates on the effect of delphinidin. Indeed, in T cells from non-MetS patients, delphinidin inhibited not only IL-2 but also ROR γ t and FOXP3, all of which are targets of NFAT. Thus, delphinidin inhibited some, but not all, of NFAT target genes, such as T-bet and GATA3, in T cells from non-MetS patients. However, in T cells from MetS, delphinidin was not able to inhibit any of the targets tested including T-bet, GATA3, ROR γ t and FOXP3, except for IL-2. Thus, the mechanism by which delphinidin is still able to inhibit IL-2 secretion in T cells from MetS patients might be due to a mechanism independent to NFAT activation.

Despite the fact that the patients with one or two MetS criteria (non-MetS patients) cannot be classified as MetS patients, they can be classified as patients with cardiovascular diseases risk factors. Thus, delphinidin can decrease T cell proliferation and modulate T cell differentiation in healthy subjects and in patients with cardiovascular diseases risk factors.

Taken together, our results suggest that delphinidin might be an immuno-modulatory and anti-inflammatory agent that can alter T lymphocyte proliferation and differentiation. The present study identifies ER α as one of key receptor transducing immuno-modulatory effect exerted by delphinidin. In addition to its preventive immunomodulatory effects in healthy subjects, delphinidin may have beneficial effects on processes leading to chronic inflammation associated with T lymphocyte activation in patients with cardiovascular risk factors. Immuno-modulation of the immune response by delphinidin can provide an alternative or complementary approach in the treatment of chronic inflammatory metabolic disorders caused by inappropriate or excessive T lymphocyte responses.

Methods

Reagents. Delphinidin chloride was purchased from Extrasynthèse (Genay, France) and was used at 10^{-2} g/L. This concentration has been described to induce the maximal relaxing effect on *ex vivo* rat aorta¹³, to prevent angiogenesis through an inhibition of migration and proliferation^{16,17} and to inhibit endothelial apoptosis⁵¹. Delphinidin was diluted in dimethylsulfoxide (DMSO) from Sigma Aldrich (St Louis, MO). The final concentration of DMSO in experiments never exceeded 0.1%. Anti-CD3 (clone OKT3) and anti-CD28 (clone CD28.2) human antibodies were purchased from BioLegend® (San Diego, CA). Histopaque®1077, Histopaque®1083, thapsigargin, Phytohemagglutinin (PHA), phorbol-12-myristate-13-acetate (PMA), ionomycin, fulvestrant, and SKF96365 were purchased from Sigma-Aldrich. Mibefradil hydrochloride was purchased from Abcam (Cambridge, UK) and trichostatin A (TSA) from Santa Cruz Biotechnology (Santa Cruz, CA). U0126 was obtained from Calbiochem (San Diego, CA). RPMI-1640, Na-pyruvate, non-essential amino-acid (NEAA) and penicillin/streptomycin were purchased from Lonza (Basel, Switzerland). Fetal bovine serum (FBS) and Fluo-4 acetoxymethyl ester (AM) were purchased from Life Technologies (Carlsbad, CA).

	Non-MetS patients	MetS patients
Number	24	46
Mean age (years)	54.9 ± 2.3	53.2 ± 1.6
Sex ratio (M/F)	11/13	24/22
BMI (kg/m ²)	30.4 ± 1.1	31.5 ± 0.8
Waist size (cm)	101.06 ± 2.52	109.7 ± 2.8*
Waist/Hips ratio	0.95 ± 0.01	1 ± 0.02*
Systolic blood pressure (mm Hg)	124.2 ± 1.8	126.4 ± 1.9
Diastolic blood pressure (mm Hg)	77.9 ± 1.6	77.2 ± 1.5
Glycemia (g/l)	1.01 ± 0.02	1.2 ± 0.04**
HBA1c (%)	5.8 ± 0.05	6.4 ± 0.15***
Total cholesterol (g/l)	2.15 ± 0.09	1.7 ± 0.08
HDL cholesterol (g/l)	0.5 ± 0.02	0.42 ± 0.004**
LDL cholesterol (g/l)	1.29 ± 0.08	1.18 ± 0.018
Triglycerides (g/l)	1.08 ± 0.07	1.6 ± 0.2*
Number of MetS components (%)		
		—
1	38	—
2	62	—
3	—	41
4	—	50
5	—	9
Treatment (%)		
Oral antidiabetic	17	52
Antihypertensive	33	58
Statins	25	40

Table 1. Baseline characteristics of non-MetS (n = 24) and MetS patients (n = 46). All patients were fasted before blood collection. All values are expressed in International System (SI) units. * $P < 0.05$, ** $P < 0.01$ and *** $P < 0.001$.

Human subjects. Human T lymphocytes were isolated from buffy coat from healthy donors obtained through the Etablissement Français du Sang (EFS Pays de la Loire, Nantes, France). Blood samples were collected and processed following standard ethical procedures after obtaining written informed consent from each donor under EFS contract N° ANG 2013–03 and approval for this study by the Ethics Committee of the University Hospital of Angers (France). MetS patients were eligible for inclusion, according to the European definition of the International Diabetes Federation (IDF)⁵², when they had at least three criteria out of the five following: (i) a waist circumference ≥ 94 or 80 cm for men and women, respectively; (ii) high systolic and diastolic pressures $\geq 130/85$ mm Hg or antihypertensive treatment; (iii) fasting glycemia ≥ 1.0 g/L or anti-diabetic treatment; (iv) triglycerides ≥ 1.5 g/L and (v) high-density lipoprotein (HDL) < 0.4 g/L in men or < 0.5 g/L in women or cholesterol-lowering drug treatment. Patients were classed on two groups depending of the number of MetS criteria that they displayed: (i) patients with one or two criteria (non-MetS patients), and (ii) patients with more than 3 criteria (MetS patients). Non-MetS and MetS patients from the METABOL cohort were included at the Department of Endocrinology and Nutrition of the University Hospital of Angers (NCT 00997165). See Table 1 for clinical parameters.

Mice. Animal study was carried out using approved institutional protocols (CEEA.2011.40) and was conformed the Guide for the Care and Use of Laboratory Animals published by U.S. National Institutes of Health (NIH Publication No. 85–23, revised 1996). C57BL/6 females ER α Wild Type (WT) or Knock-Out (KO) mice were used. They were ovariectomized at the age of 12 weeks (n = 4 animals for each group). After 7 days, blood sample was obtained from each animal by cardiac puncture following isoflurane anesthesia.

PBMC isolation and cell culture. Peripheral blood mononuclear cells (PBMCs) were isolated from blood of human subjects or mice using Histopaque[®] 1077 or Histopaque[®] 1083, respectively. Diluted blood was carefully layered onto the Histopaque and centrifuged at 400 g for 30 min. After centrifugation, the opaque interface containing mononuclear cells was collected and washed three times with PBS (pH 7.2). Cells were then resuspended in RPMI 1640 medium with 10% heat-inactivated FBS. The adherent cells were depleted by incubation in culture dish for 2 h at 37 °C in 5% CO₂ atmosphere. After isolation, PBMCs were resuspended at 10⁶ cells/mL in complete medium consisting of RPMI-1640 with ultraglutamine1 supplemented with, 1% penicillin/streptomycin, 1% NEAA, 1% Na-pyruvate and 10% FBS.

Cell phenotyping. Freshly isolated PBMCs were adjusted to a density of 1×10^6 cells/mL and labeled for 20 min at room temperature with PE- or FITC- conjugated monoclonal antibodies against CD45, CD3, CD4 and CD8 antigens (markers for leukocytes, T lymphocytes, CD4⁺ and CD8⁺ helper T cells, respectively) (Beckman Coulter, Villepinte, France). The cells were washed and resuspended in PBS, then 10,000 events were analyzed in a flow cytometer 500 MPL system and results were analyzed with CXP software (Beckman Coulter). $93.5 \pm 3.7\%$ of isolated cells were leukocytes. The purity of CD3⁺ human T lymphocytes was $77.5 \pm 7.4\%$, CD4⁺ and CD8⁺ T lymphocytes represented $59.7 \pm 5.9\%$ and $23.2 \pm 2.4\%$, respectively, of total isolated cells (Supplementary Fig. 6). Since isolated PBMCs are enriched in T cells, the term T lymphocytes will be used to describe isolated PBMCs.

Cell proliferation assay. T lymphocytes were cultured in triplicates in 96-well culture plates at 10^4 cells/well in a total volume of 0.2 mL. Cells were treated with DMSO (final concentration 0.1%, used as control), anti-CD3 plus anti-CD28 antibodies (10 $\mu\text{g}/\text{mL}$ and 5 $\mu\text{g}/\text{mL}$, respectively) in absence or in presence of delphinidin (10^{-2} g/L) and incubated in 5% CO₂-air humidified atmosphere at 37 °C for 24 and 48 h. Indeed, we have performed a proliferation test using PHA for 24, 48 and 72 h to choose the most appropriate incubation time. Our results showed that, when stimulated with PHA, the number of T cells proliferating peaked at 48 h, under the experimental condition used. The ability of PHA to induce T cell proliferation after 72 h of treatment and that of delphinidin to abrogate the response were identical than those obtained at 48 h (data not shown). Proliferation rate was assessed by using CyQUANT[®] NF Cell Proliferation Assay Kit (Life Technologies, Carlsbad, CA) according to the manufacturer's instruction. Stimulation was also induced in the presence of PHA (5 $\mu\text{g}/\text{mL}$) or PMA (10 ng/mL) plus ionomycin (1 μM). To assess the potential implication of SOCE, HDAC and ER in delphinidin effects, T cells were pre-incubated for 30 min prior to stimulation by SOCE inhibitor (SKF96365, 10 μM), HDAC inhibitor (Trichostatin A, 100 nM) or nonselective ER antagonist (fulvestrant, 100 nM), respectively. The inhibition of proliferation by delphinidin was calculated by determining the decrease in cell proliferation when T cells were treated with PHA and delphinidin compared to PHA alone.

Cell cycle analysis. T lymphocytes were cultured in 12-well culture plates at 10^6 cells/mL in a total volume of 2 mL. Then, they were treated with PHA (5 $\mu\text{g}/\text{mL}$) in absence or in presence of delphinidin (10^{-2} g/L) for 48 h. After treatment, cells were washed twice in PBS and 0.2 mL of nuclear isolation medium (50 $\mu\text{g}/\text{mL}$ propidium iodide, 0.6% NP-40, 100 $\mu\text{g}/\text{mL}$ RNase, in PBS) was added. Cells were then incubated (1 h) at room temperature in the dark before addition of 0.2 mL PBS and analyzed by flow cytometry. The distribution of cells in G₀/G₁, S and G₂/M phases was determined using CXP analysis software (Beckman Coulter).

Measurement of [Ca²⁺]_i. Isolated T lymphocytes were loaded with fluorescent Ca²⁺ indicator dye Fluo-4 AM (3 μM) (40 min at 37 °C in the dark in complete culture medium). The cells were then washed twice and suspended in physiological salt solution (PSS), pH 7.4, (composition in mM: NaCl 119, KCl 4.75, CaCl₂ 1.25, MgSO₄ 1.17, KH₂PO₄ 1.18, NaHCO₃ 25, glucose 11). The cells were then transferred to opaque 96-well culture plate and stimulated with thapsigargin (1 μM), delphinidin (10^{-2} g/L), or both. [Ca²⁺]_i was determined by fluorometric reading during 20 min performed with Mithras LB 940 Multimode Microplate Reader (Berthold Technologies), and the method of Grynkiewicz *et al.*⁵³ was used to calibrate the *in vitro* [Ca²⁺]_i as previously described¹⁵. For Ca²⁺-free experiments, CaCl₂ was omitted from PSS and 0.5 mM EGTA was added 10 min before measurement. To assess Ca²⁺ release from intracellular stores, cells were stimulated, as mentioned above, in free-Ca²⁺ PSS and the Ca²⁺ release from intracellular stores was followed for 20 min. Thereafter, CaCl₂ (1.25 mM) was added to obtain an influx of extracellular Ca²⁺. The potential implication of SOCE, HDAC and ER in delphinidin effects was tested by incubating cells for 10 min prior to stimulation by SKF96365 (10 μM), Trichostatin A (100 nM) or Fulvestrant (100 nM), respectively, then the previous experimental protocol was repeated. Also, the implication of voltage-operated Ca²⁺ channels was studied by using mibefradil (3 μM) at maximally active concentration.

Western blot. After treatment, T lymphocytes were harvested, washed twice in PBS and lysed with ice-cold RIPA buffer containing protease inhibitor on ice for 15 min. The lysates were centrifuged at 15,000 g for 15 min at 4 °C. The supernatants were collected and quantified for proteins concentration. Twenty-five μg proteins were separated on NuPAGE[™] 4–12% Bis-Tris gels (Life Technologies, Carlsbad, CA). The separated proteins were transferred onto nitrocellulose membranes (GE Healthcare, Pittsburg, PA) and blotted according to standard procedures. Blots were probed with phosphorylated or total-ERK1/2 antibodies (Cell Signaling Technology). Monoclonal anti- β -actin antibody (Sigma-Aldrich) was used to visualize protein gel loading. Membranes were then incubated with the appropriate horseradish peroxidase-conjugated secondary antibodies. Protein-antibody complexes were detected by enhanced chemiluminescence method using SuperSignal[™] West Femto Maximum Sensitivity Substrate (Thermo Scientific) with a Chemi-Smart 5000 imager system (Vilber-Lourmat, Marne-la-Vallée, France). Blots were quantified by densitometry using ImageJ software.

NFAT activation assay. T lymphocytes treated with appropriate stimulus were harvested, washed twice in PBS and nuclear extracts were prepared as previously described⁵⁴. Cells were resuspended in 200 μL of Buffer A containing 10 mM HEPES (pH 7.9), 1.5 mM MgCl₂, 10 mM KCl, with protease and phosphatase inhibitors mixture. Cells were lysed on ice for 15 min and centrifuged at 1,000 g for 10 min at 4 °C. The supernatant was saved as cytosolic fraction. The nuclear pellet was resuspended into 100 μL of Buffer B containing 20 mM HEPES (pH 7.9), 25% glycerol, 420 mM NaCl, 1.5 mM MgCl₂, 0.2 mM EDTA with protease and phosphatase inhibitors mixture. Then, samples were incubated on ice for 30 min followed by brief sonication and centrifugation at 15,000 g for 30 min at 4 °C. The supernatant containing the nuclear extracts was collected and the protein concentration was quantified. Fifteen μg of nuclear extracts were tested for the NFAT activation using TransAM[®] NFATc1 transcription factor kit (Active Motif, Carlsbad, CA) according to the manufacturer's instruction.

Intracellular transcription factors and cytokines staining. Staining of transcription factors was performed on T cells stimulated for 24 h with delphinidin (10^{-2} g/L), PHA (5 μ g/mL) or both. Cells were fixed and permeabilized using fixation and permeabilization buffers, respectively (BioLegend) according to the manufacturer's instructions, then they were stained for 45 min with FITC-conjugated anti-T-bet Ab, PE-conjugated anti-GATA3 Ab, FITC-conjugated anti-FOXP3 Ab (BioLegend) and PE-conjugated anti-ROR γ t Ab (Milteny Biotec GmbH, Bergisch Gladbach, Germany). The cells were then analyzed by flow cytometry (Beckman Coulter) and data were analyzed with Flowing Software 2.

Alternatively, intracellular production of IFN γ , IL-4, IL-17A and IL-10 (produced by Th1, Th2, Th17 and Treg, respectively), in addition to IL-2 was analyzed in T cells. For this purpose, T cells were stimulated for 5 h with delphinidin (10^{-2} g/L), PMA (50 ng/mL) plus ionomycin (1 μ g/mL), or both, in the presence of 5 μ g/mL brefeldin A (BFA) (BioLegend) for the final 3 h of culture. BFA leads to the accumulation of most cytokines inside the cell by blocking transport processes during cell activation⁵⁵. FITC-conjugated anti-human IL-2 Ab, PE/Cy7-conjugated anti-human IFN γ Ab, APC-conjugated anti-human IL-4 Ab, FITC-conjugated anti-human IL-17A Ab and APC-conjugated anti-human IL-10 Ab (BioLegend) were used to stain cytokines. Cells were then washed and data were acquired using MACSQuant Analyzer and analyzed with MACSQuantify™ Software (Milteny Biotec).

RNA isolation and analysis of transcription factors expression. T lymphocytes isolated from non-MetS and MetS patients were treated with DMSO (used as control), PHA (5 μ g/mL) in absence or in presence of delphinidin (10^{-2} g/L) and incubated in 5% CO₂-air humidified atmosphere at 37 °C for 24 h. Cells were collected and stored at -80 °C until analysis. Total cellular RNA was extracted and purified using RNeasy Micro Kit (QIAGEN) then treated with RNase-free DNase I (QIAGEN) and reverse transcribed with SuperScript™ II Reverse Transcriptase (Invitrogen) according to the manufacturer's instructions. Quantitative analysis of expression of T-bet, GATA3, ROR γ t and FOXP3 genes was performed using LightCycler® 480 System (Roche) in 384-well optical plates with Maxima SYBR Green qPCR Master Mix (ThermoFisher Scientific) according to the manufacturer's instructions. The PCR primers were provided by Eurofins MWG. Samples were analyzed in duplicate and relative expression levels of target genes were normalized to expression of RPL13a.

Cytokines measurement. T lymphocytes isolated from non-MetS and MetS patients were treated with DMSO (used as control), PHA (5 μ g/mL) in absence or in presence of delphinidin (10^{-2} g/L) and incubated in 5% CO₂-air humidified atmosphere at 37 °C for 24 h. Supernatants were collected and stored at -80 °C until analysis. Levels of IL-2, IFN γ , IL-4, IL-17A, IL-10 and IL-6 in supernatants were analyzed using Human Magnetic Luminex® Screening Assay (R&D Systems, France) on Bio-Plex 200 System (Bio-Rad). Manufacturer-specified limits of detection were 2.23, 1.27, 4.46, 1.10, 0.30 and 1.11 pg/mL for IL-2, IFN γ , IL-4, IL-17A, IL-10 and IL-6, respectively. The percent inhibition of IL-17 production by delphinidin was calculated by determining the decrease in IL-17 production when T cells were treated with PHA and delphinidin compared to PHA alone.

Statistical analysis. Data were expressed as means \pm SEM. *n* refers to the number of experiments. Statistical analyses were performed with Graph-Pad Prism Software Version 5.0 using non-parametric Mann-Whitney test. *p* < 0.05 was considered statistically significant.

References

- Monteiro, R. & Azevedo, I. Chronic inflammation in obesity and the metabolic syndrome. *Mediators Inflamm.* **2010**, 1–10 (2010).
- Paoletti, R., Bolego, C., Poli, A. & Cignarella, A. Metabolic syndrome, inflammation and atherosclerosis. *Vasc. Health Risk Manag.* **2**, 145–152 (2006).
- Esser, N., Legrand-Poels, S., Piette, J., Scheen, A. J. & Paquot, N. Inflammation as a link between obesity, metabolic syndrome and type 2 diabetes. *Diabetes Res. Clin. Pract.* **105**, 141–150 (2014).
- Gerriets, V. A. & MacIver, N. J. Role of T cells in malnutrition and obesity. *Front. Immunol.* **5**, 379 (2014).
- Wolf, D. *et al.* Coinhibitory suppression of T cell activation by CD40 protects against obesity and adipose tissue inflammation in mice. *Circulation* **129**, 2414–2425 (2014).
- Yasuda, T. & Kurosaki, T. Regulation of lymphocyte fate by Ras/ERK signals. *Cell Cycle* **7**, 3634–3640 (2008).
- Hogan, P. G., Lewis, R. S. & Rao, A. Molecular basis of calcium signaling in lymphocytes: STIM and ORAI. *Annu. Rev. Immunol.* **28**, 491–533 (2010).
- Grabiec, A. M., Tak, P. P. & Reedquist, K. A. Function of histone deacetylase inhibitors in inflammation. *Crit. Rev. Immunol.* **31**, 233–263 (2011).
- Macian, F. NFAT proteins: key regulators of T-cell development and function. *Nat. Rev. Immunol.* **5**, 472–484 (2005).
- Rincón, M., Flavell, R. A. & Davis, R. J. Signal transduction by MAP kinases in T lymphocytes. *Oncogene* **20**, 2490–2497 (2001).
- Andriantsitohaina, R. *et al.* Molecular mechanisms of the cardiovascular protective effects of polyphenols. *Br. J. Nutr.* **108**, 1532–1549 (2012).
- Cassidy, A. *et al.* Higher dietary anthocyanin and flavonol intakes are associated with anti-inflammatory effects in a population of US adults. *Am. J. Clin. Nutr.* **102**, 172–181 (2015).
- Andriambelosen, E. *et al.* Natural dietary polyphenolic compounds cause endothelium-dependent vasorelaxation in rat thoracic aorta. *J. Nutr.* **128**, 2324–2333 (1998).
- Chalopin, M. *et al.* Estrogen receptor alpha as a key target of red wine polyphenols action on the endothelium. *PLoS One* **5**, e8554 (2010).
- Martin, S., Andriambelosen, E., Takeda, K. & Andriantsitohaina, R. Red wine polyphenols increase calcium in bovine aortic endothelial cells: a basis to elucidate signalling pathways leading to nitric oxide production. *Br. J. Pharmacol.* **135**, 1579–1587 (2002).
- Favot, L., Martin, S., Keravis, T., Andriantsitohaina, R. & Lugnier, C. Involvement of cyclin-dependent pathway in the inhibitory effect of delphinidin on angiogenesis. *Cardiovasc. Res.* **59**, 479–487 (2003).
- Martin, S., Favot, L., Matz, R., Lugnier, C. & Andriantsitohaina, R. Delphinidin inhibits endothelial cell proliferation and cell cycle progression through a transient activation of ERK-1/-2. *Biochem. Pharmacol.* **65**, 669–675 (2003).
- Byun, J.-K. *et al.* Epigallocatechin-3-gallate ameliorates both obesity and autoinflammatory arthritis aggravated by obesity by altering the balance among CD4+ T-cell subsets. *Immunol. Lett.* **157**, 51–59 (2014).
- Zou, T. *et al.* Resveratrol Inhibits CD4+ T cell activation by enhancing the expression and activity of Sirt1. *PLoS One* **8**, e75139 (2013).

20. Jara, E. *et al.* Delphinidin activates NFAT and induces IL-2 production through SOCE in T cells. *Cell Biochem. Biophys.* **68**, 497–509 (2014).
21. Seong, A.-R. *et al.* Delphinidin, a specific inhibitor of histone acetyltransferase, suppresses inflammatory signaling via prevention of NF- κ B acetylation in fibroblast-like synoviocyte MH7A cells. *Biochem. Biophys. Res. Commun.* **410**, 581–586 (2011).
22. D'Souza, W. N., Chang, C.-F., Fischer, A. M., Li, M. & Hedrick, S. M. The Erk2 MAPK regulates CD8 T cell proliferation and survival. *J. Immunol.* **181**, 7617–7629 (2008).
23. Teng, Z., Xing, F., Wang, T. & Li, L. [Effect of extracellular-signal regulated kinase 1/2 specific repressor PD98059 on murine lymphocyte proliferation]. *Xi Bao Yu Fen Zi Mian Yi Xue Za Zhi Chin.* **23**, 102–105 (2007).
24. Zhang, W. & Liu, H. T. MAPK signal pathways in the regulation of cell proliferation in mammalian cells. *Cell Res.* **12**, 9–18 (2002).
25. Schwarz, E. C. *et al.* Calcium dependence of T cell proliferation following focal stimulation. *Eur. J. Immunol.* **37**, 2723–2733 (2007).
26. Feske, S. Calcium signalling in lymphocyte activation and disease. *Nat. Rev. Immunol.* **7**, 690–702 (2007).
27. Mallat, Z., Taleb, S., Ait-Oufella, H. & Tedgui, A. The role of adaptive T cell immunity in atherosclerosis. *J. Lipid Res.* **50**(Suppl), S364–369 (2009).
28. Nishimura, S. *et al.* CD8+ effector T cells contribute to macrophage recruitment and adipose tissue inflammation in obesity. *Nat. Med.* **15**, 914–920 (2009).
29. Keul, P. *et al.* The sphingosine-1-phosphate analogue FTY720 reduces atherosclerosis in apolipoprotein E-deficient mice. *Arterioscler. Thromb. Vasc. Biol.* **27**, 607–613 (2007).
30. Klingenberg, R. *et al.* Sphingosine-1-phosphate analogue FTY720 causes lymphocyte redistribution and hypercholesterolemia in ApoE-deficient mice. *Arterioscler. Thromb. Vasc. Biol.* **27**, 2392–2399 (2007).
31. Nofer, J.-R. *et al.* FTY720, a synthetic sphingosine 1 phosphate analogue, inhibits development of atherosclerosis in low-density lipoprotein receptor-deficient mice. *Circulation* **115**, 501–508 (2007).
32. von Vietinghoff, S. *et al.* Mycophenolate mofetil decreases atherosclerotic lesion size by depression of aortic T-lymphocyte and interleukin-17-mediated macrophage accumulation. *J. Am. Coll. Cardiol.* **57**, 2194–2204 (2011).
33. Ozbay, T. & Nahta, R. Delphinidin Inhibits HER2 and Erk1/2 Signaling and Suppresses Growth of HER2-Overexpressing and Triple Negative Breast Cancer Cell Lines. *Breast Cancer Basic Clin. Res.* **5**, 143–154 (2011).
34. Syed, D. N. *et al.* Delphinidin inhibits cell proliferation and invasion via modulation of Met receptor phosphorylation. *Toxicol. Appl. Pharmacol.* **231**, 52–60 (2008).
35. Wang, L.-S. & Stoner, G. D. Anthocyanins and their role in cancer prevention. *Cancer Lett.* **269**, 281–290 (2008).
36. Hock, M. *et al.* NFATc1 induction in peripheral T and B lymphocytes. *J. Immunol.* **190**, 2345–2353 (2013).
37. Serfling, E. *et al.* The role of NF-AT transcription factors in T cell activation and differentiation. *Biochim. Biophys. Acta* **1498**, 1–18 (2000).
38. Legube, G. & Trouche, D. Regulating histone acetyltransferases and deacetylases. *EMBO Rep.* **4**, 944–947 (2003).
39. Liu, J. O. Calmodulin-dependent phosphatase, kinases, and transcriptional corepressors involved in T-cell activation. *Immunol. Rev.* **228**, 184–198 (2009).
40. Skov, S. *et al.* Histone deacetylase inhibitors: a new class of immunosuppressors targeting a novel signal pathway essential for CD154 expression. *Blood* **101**, 1430–1438 (2003).
41. Wei, Q., Yu, L., Deng, W. & Ye, J. [Effect of trichostatin A on proliferation and interleukin-2 expression of mouse T cells in mixed lymphocyte culture]. *Nan Fang Yi Ke Da Xue Xue Bao* **28**, 467–469 (2008).
42. Ohl, K. & Tenbrock, K. Inflammatory cytokines in systemic lupus erythematosus. *J. Biomed. Biotechnol.* **2011**, 432595 (2011).
43. Rider, V. *et al.* Differential expression of estrogen receptors in women with systemic lupus erythematosus. *J. Rheumatol.* **33**, 1093–1101 (2006).
44. Schneider, C. P. *et al.* The aromatase inhibitor, 4-hydroxyandrostenedione, restores immune responses following trauma-hemorrhage in males and decreases mortality from subsequent sepsis. *Shock* **14**, 347–353 (2000).
45. Holm, A., Andersson, K. E., Nordström, I., Hellstrand, P. & Nilsson, B.-O. Down-regulation of endothelial cell estrogen receptor expression by the inflammation promoter LPS. *Mol. Cell. Endocrinol.* **319**, 8–13 (2010).
46. Puri, J., Hutchins, B., Bellinger, L. L. & Kramer, P. R. Estrogen and inflammation modulate estrogen receptor alpha expression in specific tissues of the temporomandibular joint. *Reprod. Biol. Endocrinol.* **7**, 155 (2009).
47. Stoner, M. *et al.* Hypoxia induces proteasome-dependent degradation of estrogen receptor alpha in ZR-75 breast cancer cells. *Mol. Endocrinol.* **16**, 2231–2242 (2002).
48. Johnson, A. R., Milner, J. J. & Makowski, L. The inflammation highway: metabolism accelerates inflammatory traffic in obesity. *Immunol. Rev.* **249**, 218–238 (2012).
49. Gajewski, T. F., Schell, S. R. & Fitch, F. W. Evidence implicating utilization of different T cell receptor-associated signaling pathways by TH1 and TH2 clones. *J. Immunol.* **144**, 4110–4120 (1990).
50. Hermann-Kleiter, N. & Baier, G. NFAT pulls the strings during CD4+ T helper cell effector functions. *Blood* **115**, 2989–97 (2010).
51. Martin, S., Giannone, G., Andriantsitohaina, R. & Martinez, M. C. Delphinidin, an active compound of red wine, inhibits endothelial cell apoptosis via nitric oxide pathway and regulation of calcium homeostasis. *Br. J. Pharmacol.* **139**, 1095–1102 (2003).
52. Alberti, K. G. M. M. *et al.* Armonizing the metabolic syndrome: a joint interim statement of the International Diabetes Federation Task Force on Epidemiology and Prevention; National Heart, Lung, and Blood Institute; American Heart Association; World Heart Federation; International Atherosclerosis Society; and International Association for the Study of Obesity. *Circulation* **120**, 1640–1645 (2009).
53. Gryniewicz, G., Poenie, M. & Tsien, R. Y. A new generation of Ca²⁺ indicators with greatly improved fluorescence properties. *J. Biol. Chem.* **260**, 3440–3450 (1985).
54. Wong, H. K., Kammer, G. M., Dennis, G. & Tsokos, G. C. Abnormal NF-kappa B activity in T lymphocytes from patients with systemic lupus erythematosus is associated with decreased p65-ReIA protein expression. *J. Immunol.* **163**, 1682–1689 (1999).
55. Jung, T., Schauer, U., Heusser, C., Neumann, C. & Rieger, C. Detection of intracellular cytokines by flow cytometry. *J. Immunol. Methods* **159**, 197–207 (1993).

Acknowledgements

We thank Jérôme Cayon and Catherine Guillet from PACeM (Plate-forme d'Analyses Cellulaire et Moléculaire) for technical assistance in RT-qPCR and intracellular cytokine staining experiences. We thank Simon Blanchard for technical assistance with Luminex[®] technology. We thank the staff of Centre Hospitalo-Universitaire d'Angers for the inclusion of patients and analysis of clinical data of METABOL cohort. We thank also Mireille Wertheimer for taking care of animals. We sincerely thank Dr Pauline Soulas-Sprauel for its expertise and the critical reading of the manuscript, and Dr Ziad Mallat for his critical remarks. Ousama Dayoub is recipient of a doctoral fellowship from the Atomic Energy Commission of Syria.

Author Contributions

O.D., S.L.L., R.S., N.C. and G.H. designed experiments, researched data; S.D., F.G., and J.B. recruited patients; O.D., S.L.L., and M.C.M. wrote and reviewed the manuscript; R.A. designed experiments, wrote, reviewed edited the manuscript.

Additional Information

Supplementary information accompanies this paper at doi:[10.1038/s41598-017-09933-4](https://doi.org/10.1038/s41598-017-09933-4)

Competing Interests: The authors declare that they have no competing interests.

Publisher's note: Springer Nature remains neutral with regard to jurisdictional claims in published maps and institutional affiliations.



Open Access This article is licensed under a Creative Commons Attribution 4.0 International License, which permits use, sharing, adaptation, distribution and reproduction in any medium or format, as long as you give appropriate credit to the original author(s) and the source, provide a link to the Creative Commons license, and indicate if changes were made. The images or other third party material in this article are included in the article's Creative Commons license, unless indicated otherwise in a credit line to the material. If material is not included in the article's Creative Commons license and your intended use is not permitted by statutory regulation or exceeds the permitted use, you will need to obtain permission directly from the copyright holder. To view a copy of this license, visit <http://creativecommons.org/licenses/by/4.0/>.

© The Author(s) 2017